

Electronic Supplementary Information

**Enhanced catalysis of ZnO-CuO-Co₃O₄ composites by
mechanochemical method for effective Fenton-like dye removal: The
generation and catalytic mechanism of various superficial active sites**

Xueping Li^a, Kangkang Miao^a, Sifan Guo^a, Nan Wang^a, Qian Zhuang^a, Huaming Qian^a, Xiaolin Luo^{a,*}, Guodong Feng^{b,*}

^a*Key Laboratory of Advanced Molecular Engineering Materials, College of Chemistry and Chemical Engineering, Engineering Research Center for Titanium Based Functional Materials and Devices in Universities of Shaanxi Province, Baoji University of Arts and Sciences, Baoji 721013, P. R. China*

^b*Xi'an Key Laboratory of Sustainable Energy Materials Chemistry, College of Chemistry, Xi'an Jiaotong University, Xi'an 710049, P. R. China*

1. Supplementary Methods

1.1 Chemicals

Copper(II) acetate monohydrate [Cu(Ac)₂·H₂O], zinc acetate dihydrate [Zn(Ac)₂·2H₂O], cobalt(II) acetate tetrahydrate [Co(Ac)₂·4H₂O], H₂O₂ (30%), methyl orange (MO), orange IV (Or IV), methylene blue (MB), rhodamine B (Rh B), tetracycline (TC), 4-chlorophenol (4-CP), bisphenol A (BPA) and humic acid (HA) were purchased from Sinopharm company. 5-tert-butoxycarbonyl 5-methyl-1-pyrroline N-oxide (BMPO) and dimethyl pyridine N-oxide (DMPO) were purchased from Aladdin industrial company. All chemicals were used directly in the experiment.

1.2 Partial characterization of the Fenton-like degradation of dye wastewater

The stability tests of the sample III were carried out as the following procedure. Considering the catalyst loss in the experiment, 100 mg instead of 25 mg catalyst was used in the Fenton-like treatment of MO/MB wastewater under other fixed conditions. After each treatment, the catalyst was recycled through high-speed centrifugation and directly reused in the next experiment. When the operation was performed five times, the residual solid was separated and dried at 110 °C for 6 h. About 70 mg of the pristine or recycled catalysts were detected by XRD to analyze their crystallographic variation.

The degradation of HA and TC was executed following the same procedure as that of MO treatment except the different maximum absorption wavelengths. In the degradation of 4-CP and BPA, the composition of the effluents was analysed by high-performance liquid chromatography (HPLC, 1100, Agilent) with a mobile phase as $V(\text{methyl alcohol}) : V(\text{H}_2\text{O}) = 15 : 85$.

5.0 mg of the samples were dispersed in 0.25 mL of ethyl alcohol, and the obtained slurry was uniformly dropped onto a 1×1.5 cm² FTO glass to cover the area of 1×1 cm². The FTO glass was then dried in a drying oven at 60 °C for 6 h. A standard three-electrode setup was used, the FTO glass coated with the samples as working electrode, a Pt electrode as counter electrode, and Ag/AgCl electrode as reference electrode. The three electrodes were inserted in a quartz cell filled with 0.5 M Na₂SO₄ electrolyte for electrochemical measurements by a Solartron ModulabXM electrochemical station. Linear sweep voltammetry (LSV) for the samples were measured with a scan rate of 10 mV·s⁻¹, and the potential ranged from 0 V to -1.0 V (vs. RHE). The *i-t* curves

were analyzed by using the same electrodes.

For electron spin resonance (ESR) spectra measurement, 25 mg catalyst was dispersed in 50 mL aqueous (for $\cdot\text{OH}$) or methanol (for $\cdot\text{O}_2^-$) solution. 150 μL H_2O_2 (30%) was added into above solution under vigorous stirring to simulate the Fenton-like system. Then, 10 μL of DMPO or BMPO ($250\text{ mmol}\cdot\text{L}^{-1}$) was added into the previous solution, and the obtained system was detected by a ESR spectrometer (A300, Bruker).

Total organic carbon (TOC) was determined by a Shimadzu TOC-VCPH analyzer using high-temperature combustion. The TOC value was automatically calculated by TC minus IC.

Hydroxy radical detection was carried out by fluorescence spectrometry. 50 mg catalyst was dispersed in a mixed aqueous solution (25 mL) containing terephthalic acid ($0.5\text{ mmol}\cdot\text{L}^{-1}$) and NaOH ($2.0\text{ mmol}\cdot\text{L}^{-1}$). The reaction system was heated at a constant temperature as $50\text{ }^\circ\text{C}$. Then, 0.15 mL H_2O_2 aqueous solution was added into the previous system with magnetic stirring for 1.0 min. Fluorescence spectra of the solution after being diluted twice was determined by a RF-5301PC series fluorescence spectrophotometer with an excitation wavelength as 315 nm.

The degradation intermediates of MO or MB were identified by gas chromatograph-mass spectrometry (GC-MS, Agilent) equipped with a HP-5 MS column ($30\text{ m} \times 0.25\text{ mm} \times 0.25\text{ }\mu\text{m}$). The suspension at a reaction time of 10, 25 and 45 mins was filtered, and 5 mL of filtrate was acidized to about $\text{pH}=2$ and extracted with 3 mL ethyl acetate four times to obtain the extracts in a 10 mL separating funnel. Then the extract solution was dehydrated by 2 g of anhydrous magnesium sulfate for 20 mins. The ethyl acetate was removed using a termovap sample concentrator to approximately 1 mL. Last, 0.1 mL hexamethyl-disilazane was added to the derivate for at least 1 hour at room temperature. The derivation solution was transferred into a 1.5 mL chromatographic bottle for GC-MS analysis. The GC parameters are listed as follows: injector temperature of $250\text{ }^\circ\text{C}$, an initial oven temperature of $40\text{ }^\circ\text{C}$ for 2 mins, and then a programmed increased to $300\text{ }^\circ\text{C}$ at the rate of $10\text{ }^\circ\text{C}/\text{min}$ and held for 2 mins.

1.3 Characterization of the oxidative species generated in the Fenton-like system

Hydroxy radical detection was carried out by fluorescence spectrometry. 25 mg catalyst was dispersed in a mixed aqueous solution (50 mL) containing terephthalic acid ($0.5\text{ mmol}\cdot\text{L}^{-1}$) and NaOH ($2.0\text{ mmol}\cdot\text{L}^{-1}$). Then, 0.15 mL H_2O_2 aqueous solution was added into the previous system with magnetic stirring for 1.0 min. Fluorescence spectra of the solution after being diluted for 10

times was determined at a certain time by a RF-5301PC series fluorescence spectrophotometer with an excitation wavelength as 315 nm. The relative concentration of the formed hydroxy radical was calculated by using luminescent intensity of the system without the catalyst as a reference.

25 mg catalyst was dispersed in a 9,10-anthracenediyl-bis(methylene) dimalonic acid (ABDA, $0.05 \text{ mmol}\cdot\text{L}^{-1}$) dimethylsulfoxide-water solution ($V_{\text{DMSO}} : V_{\text{H}_2\text{O}} = 1:100$). $0.15 \text{ mL H}_2\text{O}_2$ aqueous solution was added into the previous system with magnetic stirring. At a certain of time, 1 mL of aliquots was taken out and separated by filter membrane. The filtrate was immediately analysed by a UV-vis spectrometer (U-3900, Hitachi) at an absorption wavelength near 380 nm . The absorbance decline relative to the initial value at 380 nm was recorded to indicate the decomposition rates of ABDA ($^1\text{O}_2$ generation rate). The relative concentration of $^1\text{O}_2$ was calculated by using the absorbance decline of the system without the catalyst as a reference.

1.4 Curve fitting of XPS data

Curve fitting of Co 2p, Cu 2p and O 1s XPS spectra was carried out by a professional software (Thermo Avantage). Bonding energies of all XPS peaks were firstly calibrated by contaminative C 1s (284.8 eV). The bonding energies of Zn 2p, Co 2p, Cu 2p and O 1s were established by using “Handbook of The Elements and Native Oxides” edited by 1999 XPS International as reference. In view of spin-orbit splitting, 2p characteristic XPS levels were extracted as two kinds of the related peaks, namely, $2p_{3/2}$ and $2p_{1/2}$, and the area ratio between $2p_{3/2}$ and $2p_{1/2}$ components was fixed as 1:2 in the curve fitting. The background analysis was operated by the software automatically, and curve fitting was optimized by the software intelligently for three times to achieve an advisable fitting degree. As a result, full width at half maximum (FWHM) of the fitting peaks was lower than 2.7 eV , and the separations between the $3/2$ and $1/2$ components of the Co and Cu 2p orbitals were 15.0 and 19.7 eV , respectively.

1.5 Artemia salina cultivation and acute test

The cultivation and acute test methodology for artemia salina were designed here, according to Chinese national standard (GB/T 16310.1).

The test organisms (artemia salina) were cultured in $1.0 \text{ wt}\%$ simulated sea water with salt concentration of $0.50 \text{ g}\cdot\text{L}^{-1}$ and pH value of $7.0\sim 8.0$. The organisms were maintained at in batches for 24 hrs , with diffuse luminosity and temperature of $25 \text{ }^\circ\text{C}$ in an incubator.

MO/MB effluent samples were tested based on the exposure for a period of 24 of neonates *artemia salina*. Six test solutions from each effluent and one control were used. The dilutions were prepared with volumetric precision, in a geometric progression of ratio 2. The simulated sea water was used for dilution of effluents and as a control. The death of the organisms was judged by immobilization under any of conditions. The test was considered valid when less than 10% of the organisms showed immobilization on the control. Each solution was distributed in 4 holes of 96-well plates, with 200 μ L of test solution containing 13 organisms in each. During the test period, the organisms were kept an incubator, with the temperature of 25 °C and diffuse luminosity. The number of immobile individuals was counted after 24 hrs acute test, and the median effective concentration (EC_{50}) were calculated.

2. Supplementary results

Table S1 XRD diffraction peak location of the obtained transition metal oxidates and the sample I–III

Peak No.	ZnO	CuO	C ₀ 3O ₄	Sam. I	Sam. II	Sam. III
$2\theta^\circ$ (<i>hkl</i>)						
1			31.2 (220)	31.4 (220)	31.4 (220)	31.3 (220)
2	31.9 (100)			31.9 (110)	32.0 (110)	31.8 (110)
3		32.8 (-110)				
4	34.6 (002)			34.6 (002)	34.5 (002)	34.5 (002)
5		35.8 (002)		35.7 (002)	35.6 (002)	35.5 (002)
6	36.3 (101)			36.4 (101)	36.4 (101)	36.3 (101)
7			36.8 (311)	37.0 (311)	37.0 (311)	36.9 (311)
8			38.5 (222)			
9		39.0 (111)		39.0 (111)	38.7 (111)	38.6 (111)
10			44.8 (400)	45.0 (400)	44.9 (400)	44.8 (400)
11	47.6 (102)			47.7 (102)		47.6 (102)

12		49.1 (-202)	48.8 (-202)		
13		53.7 (020)			
14			55.7 (422)	55.8 (422)	55.8 (422)
15	56.7 (110)			56.7 (110)	56.7 (110)
16		58.5 (202)			
17			59.3 (511)	59.5 (511)	59.5 (511)
18		61.8 (-113)			
19	63.0 (103)			63.0 (103)	62.8 (103)
20			65.2 (440)	65.4 (440)	65.4 (440)
21	68.1 (112)			68.1 (112)	65.3 (440)

Table S2 The primary characteristic XRD diffraction peak intensity ratios of the obtained samples

No.	$I_{110}: I_{002}: I_{101}: I_{102}: I_{110}: I_{103}: I_{112}$ (ZnO)	$I_{-110}: I_{002}: I_{111}: I_{-202}: I_{020}: I_{202}: I_{-113}$ (CuO)	$I_{220}: I_{311}: I_{222}: I_{400}: I_{422}: I_{511}: I_{440}$ (Co ₃ O ₄)
ZnO	0.54: 0.43: 1: 0.24: 0.36: 0.33: 0.28	--	--
CuO	--	0.09: 0.91: 1: 0.29: 0.11: 0.14: 0.22	--
Co ₃ O ₄	--	--	0.35: 1: 0.10: 0.19: 0.08: 0.31: 0.36
Sam. I	0.60: 0.46: 1: 0.24: 0.33: 0.29: 0.24	0: 0.76: 1: 0.19: 0: 0: 0	0.35: 1: 0: 0.17: 0.10: 0.32: 0.38
Sam. II	0.96: 0.84: 1: 0: 0.43: 0.30: 0	0: 1: 0.87: 0: 0: 0: 0	0.40: 1: 0: 0.17: 0.09: 0.29: 0.32
Sam. III	0.73: 0.66: 1: 0.23: 0: 0.26: 0	0: 0.97: 1: 0: 0: 0: 0	0.41: 1: 0: 0.13: 0.09: 0.23: 0.27

Table S3 Comparison of the Fenton-like degradation of organic pollutants catalyzed by Co/Cu-containing catalysts

No.	Catalyst	Pollutants ^a	Reaction conditions	TOC COD	Ref.
1	Fe-Nb-Cu-Si-B alloy	MO	$c(\text{MO}) = 25 \text{ mg/L}$, 35 °C, 60 mins Ultrasonic irradiation	57%	1
2	Zr ₅₅ Cu ₃₀ Ni ₅ Al ₁₀	MO, CR, RhB, MB, AO II	$c(\text{Mixture}) = 25 \text{ mg/L}$, 45 °C, 30 mins	92%	2

3	Cu/ γ -Al ₂ O ₃ pellets	MO	$c(\text{MO}) = 30 \mu\text{M}, 20 \text{ }^\circ\text{C}$ Fixed bed reactor	74%	3
4	CuO-CeO ₂ -Co ₃ O ₄	EPE	$c(\text{EPE}) = 30 \text{ mg/L}, \text{RT}, 90 \text{ mins}$	44-55%	4
5	Cu-CoO _x	MNZ	$c(\text{MNZ}) = 10 \text{ ppm}, 50 \text{ }^\circ\text{C}, 30 \text{ mins}$	64-69%	5
6	CuO-Co ₃ O ₄ @AC	HA	$c(\text{HA}) = 100 \text{ mg/L}, 80 \text{ }^\circ\text{C}, 60 \text{ mins}$ Microwave irradiation	71%	6
7	C-g-C ₃ N ₄ /CuCo-Al ₂ O ₃	MO, Phenol, BPA	$c(\text{BPA}) = 23 \text{ mg/L}, \text{RT}, 30 \text{ mins}$	~70%	7
8	CuFeO _x /Al-MCM-41	Phenol	$c(\text{Phenol}) = 80 \text{ mg/L}, 60 \text{ }^\circ\text{C}, 120 \text{ mins}$	47%	8
9	nZVC-Cu(II)-rGO	BPA, 2-CP	$c(2\text{-CP}) = 10 \text{ mg/L}, \text{RT}, 30 \text{ mins}$	71.8%	9
10	ZnO-Co ₃ O ₄ -CuO	MO MB	$c(\text{MO/MB}) = 20 \text{ mg/L}, \text{RT}, 120 \text{ mins}$	>70%	This work

Pollutants^a: methyl orange (MO), orange IV (Or IV), methylene blue (MB), Congo red (CR), rhodamine B (RhB), 2-chlorophenol (2-CP), bisphenol A (BPA), acid orange II (AO II), Electroless plating effluent (EPE), Metronidazole (MNZ) and humic acid (HA)

Table S4 Bonding energy of the fitting peaks in XPS spectra

Sam.	Bonding energy/ eV					
	Co(III) 2p _{3/2}	Co(II) 2p _{3/2}	Cu(I) 2p _{3/2}	Cu(II) 2p _{3/2}	O _{lattice} 1s	OH 1s
I	779.6	780.7	932.7	934.1	529.9	531.9
II	779.7	780.9	933.3	934.9	530.1	532.1
III	779.8	780.9	933.0	934.5	529.9	531.9
I+H ₂ O ₂ ^a	779.8	780.8	933.0	934.3	530.0	532.0
II+H ₂ O ₂	779.8	781.0	933.0	934.5	530.0	532.0
III+H ₂ O ₂	779.7	780.7	932.7	933.9	529.8	531.9
I+10 mins ^b	779.8	780.8	932.7	934.0	530.0	531.9
II+10 mins	779.8	780.9	933.0	934.7	530.0	531.9
III+10 mins	779.6	780.6	932.7	933.9	529.8	531.7
I+30 mins ^c	779.4	780.4	932.5	934.0	529.5	531.4
II+30 mins	779.6	780.6	933.0	934.3	529.7	531.3
III+30 mins	779.6	780.6	933.3	934.5	529.9	531.3

a: the samples reacted in H₂O₂ solution for 10 mins; b: the samples recycled from the Fenton-like degradation of MO after 10 mins reaction; c: the samples recycled from the Fenton-like degradation of MO after 30 mins reaction

Table S5 Results of the acute toxicity test for artemia salina for MO/MB aqueous solution at different concentrations after 24 h exposure

Concentration (mg·L ⁻¹)	Average Immobility (%)		Average Immobility (%)	
	MO OS ^a	MO TS ^b (4 hrs)	MB OS ^a	MB TS ^b (4 hrs)
Control/0	0	0	0	0
10	48.7	41.0	45.9	34.7
20	59.0	43.6	48.7	38.4
30	61.5	56.4	50.0	42.3
40	66.7	61.5	66.7	42.3
60	76.9	64.8	73.9	47.4
Median effective concentrations (EC50%)	7.11 mg·L ⁻¹	21.2 mg·L ⁻¹	11.7 mg·L ⁻¹	150.3 mg·L ⁻¹

a: original solution; b: Treated solution

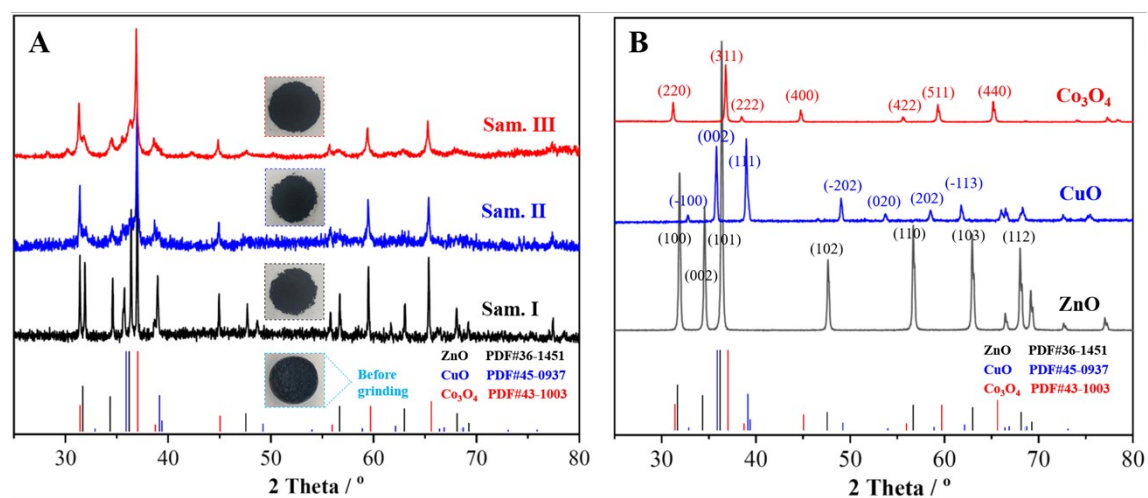


Fig. S1 XRD patterns of the samples I–III (A) and the pristine transition metal oxides (B)

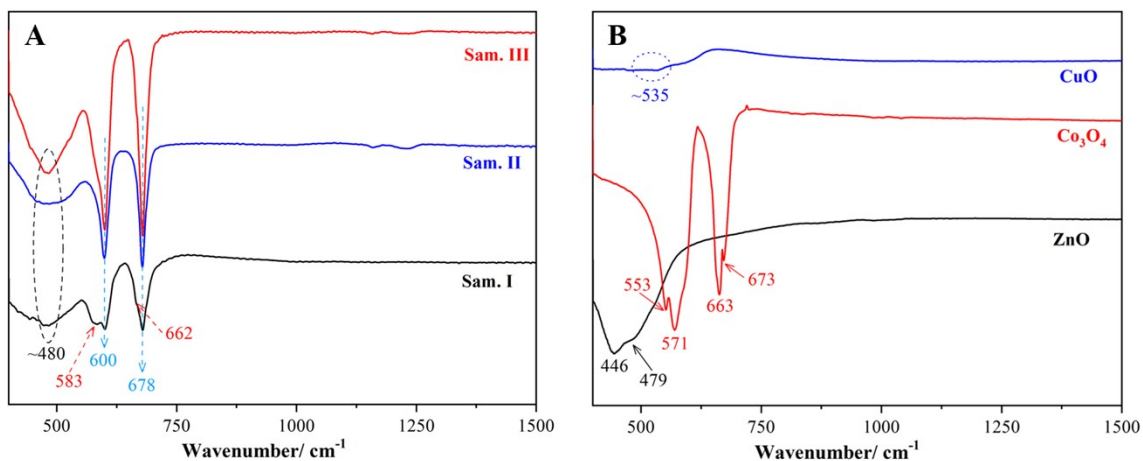


Fig. S2 FT-IR spectra of the samples I–III (A) and the pristine transition metal oxides (B)

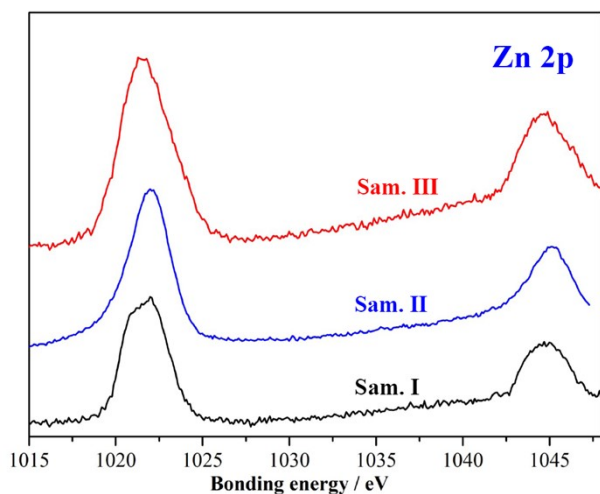


Fig. S2 Zn 2p XPS graphs of the samples

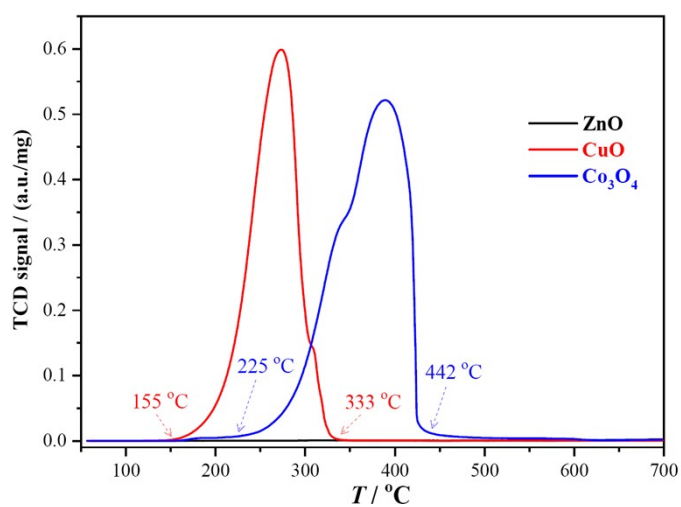


Fig. S3 H_2 -TPR curves of the pure transition metal oxides

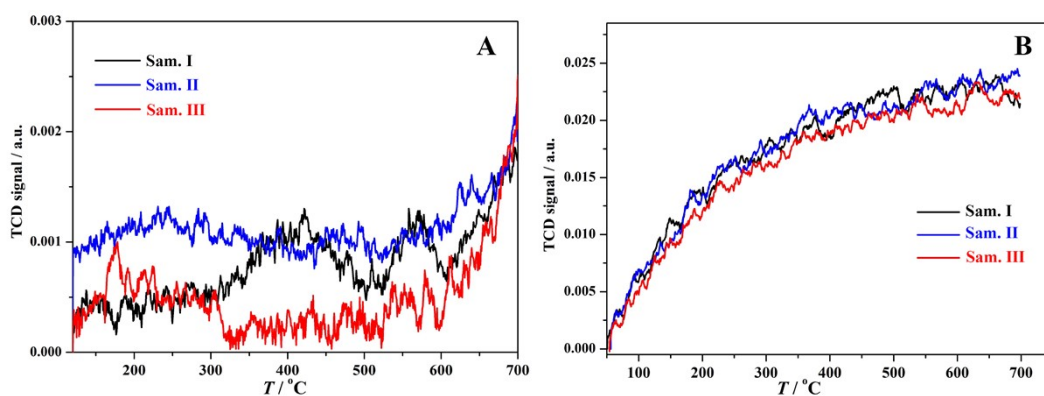


Fig. S4 Active site characterization results of the samples: (A) NH_3 -TPD curves, (B) O_2 -TPO curves

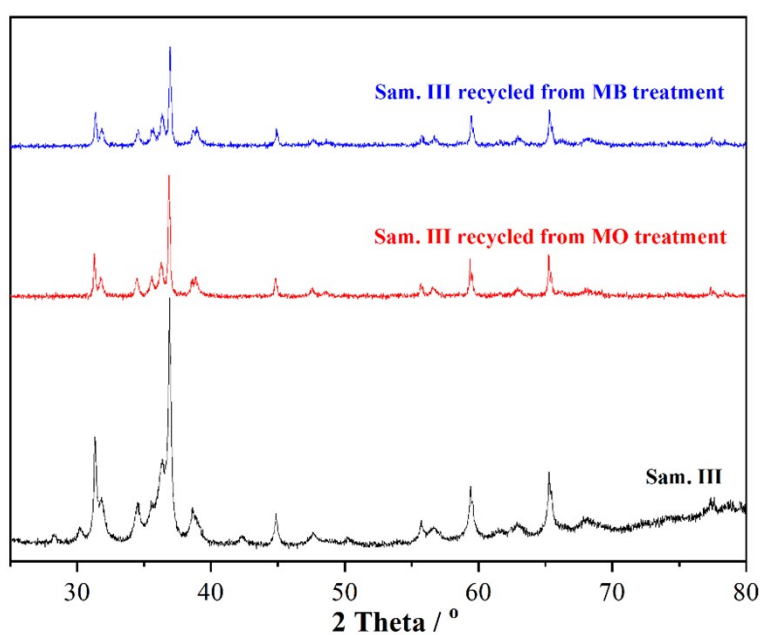


Fig. S5 XRD patterns of the samples III recycled after the Fenton-like treatment of MO/MB wastewater

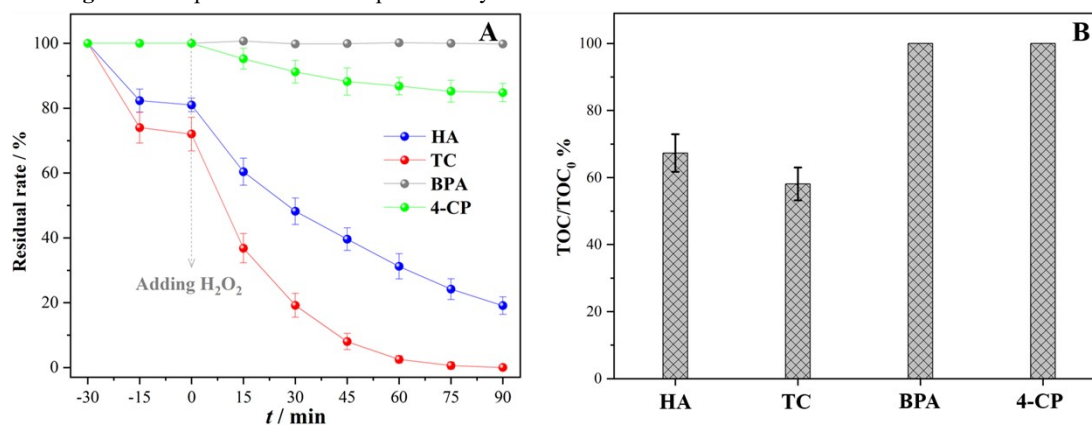


Fig. S6 Fenton-like degradation of dye-free organic pollutants catalyzed by the sample III: (A) Degradation curves, (B) TOC removal efficiency after 90 mins treatment. Reaction conditions: $[\text{Pollutant}] = 20.0 \text{ mg}\cdot\text{L}^{-1}$, $[\text{H}_2\text{O}_2] = 0.9 \text{ g}\cdot\text{L}^{-1}$, $[\text{catalyst}] = 5.0 \text{ g}\cdot\text{L}^{-1}$, room temperature

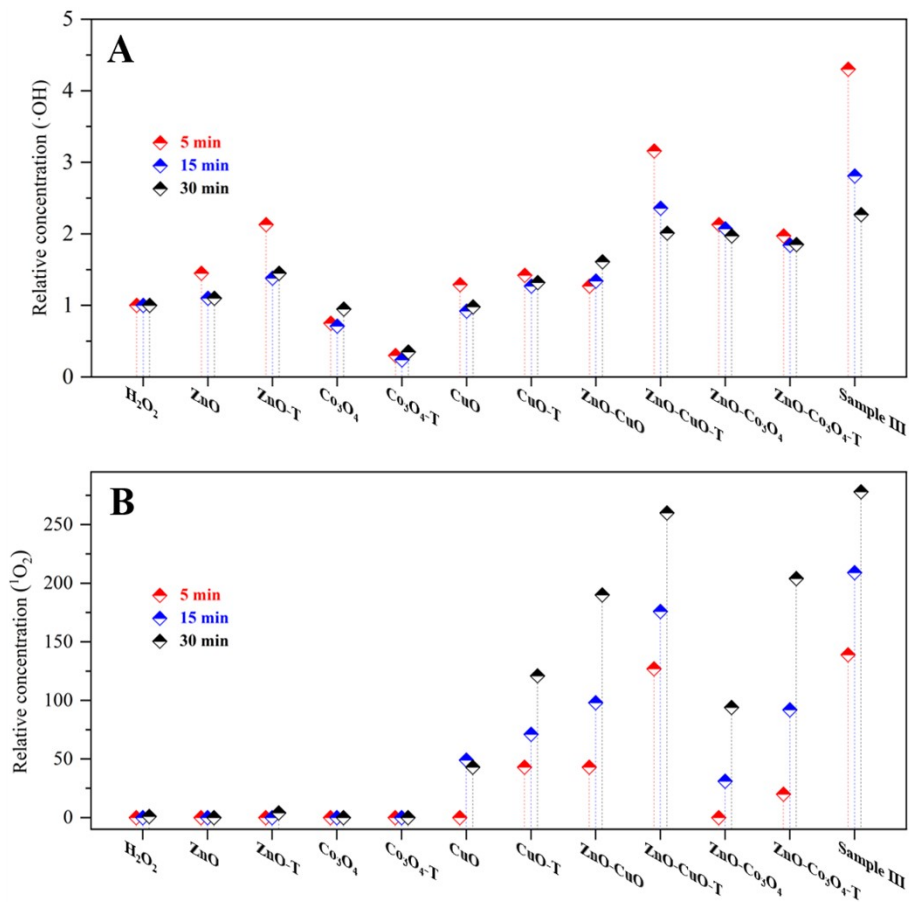


Fig. S7 Free radical studies in the Fenton-like reactions: (A) $\cdot\text{OH}$ relative concentration in various systems determined by fluorescence spectrometry of TA oxidation, (B) $^1\text{O}_2$ relative concentration in various systems determined by UV-vis spectrometry of ABDA degradation. -T: the samples treated by the high-speed vibrating ball muller as that of the sample III

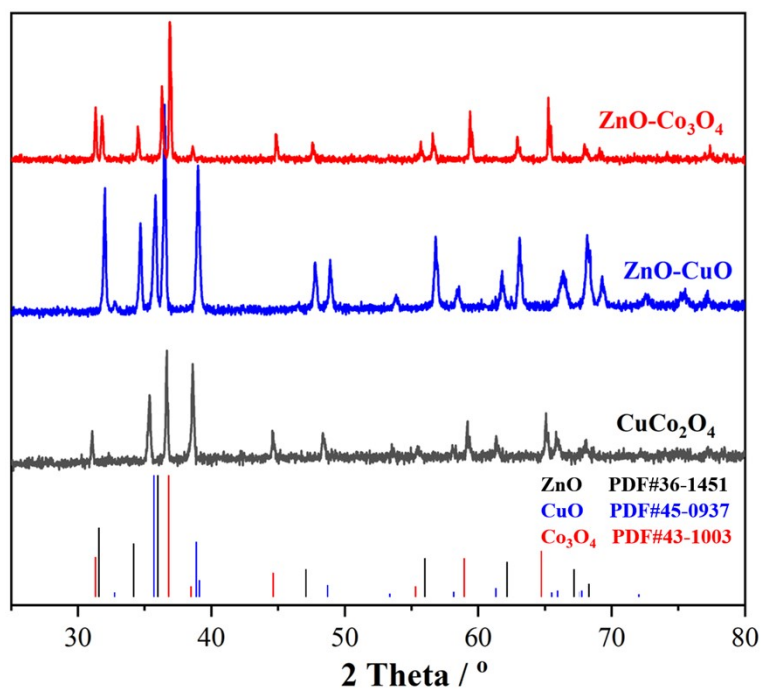


Fig. S8 XRD patterns of the synthesized binary metal oxidates

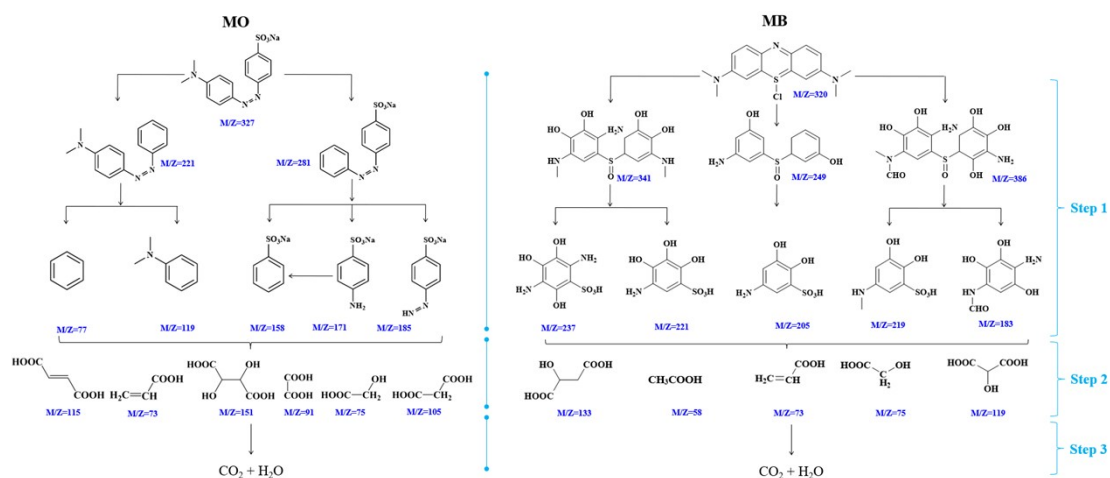


Fig. S9 The proposed pathway for the Fenton-like degradation of MO and MB basing on GC-MS data

References

- [1] L. Tan, X. Wang, S. Wang, X. Qin, L. Xiao, C. Li, S. Sun, S. Hu, Degradation of methyl orange by an ultrasonic Fenton-like process with Fe-based amorphous alloy powders, *New J. Chem.*, 2023, 47, 11723–11735.
- [2] C. Yang, C. Zhang, L. Liu, Excellent degradation performance of 3D hierarchical nanoporous structures of copper towards organic pollutants, *J. Mater. Chem. A*, 2018, 6, 20992–21002.
- [3] D. Ding, P. Tian, C. Cao, Y. Sun, J. Xu, Y. F. Han, Degradation of MO and H_2O_2 on $\text{Cu}/\gamma\text{-Al}_2\text{O}_3$ pellets in a fixed bed reactor: Kinetics and transport characteristics, *AIChE J.*, 2020, 66, 17000–17010.
- [4] X. Ji, H. Liang, S. Hu, B. Yang, K. Xiao, G. Yu, Highly efficient decomplexation of chelated nickel and copper effluent through $\text{CuO-CeO}_2\text{-Co}_3\text{O}_4$ nanocatalyst loaded on ceramic membrane, *Chemosphere*, 2023, 334, 138981–138989.
- [5] X. Guo, B. Hu, K. Wang, H. Wang, B. Li, M. Guo, Y. Tian, R. Zhang, S. Shi, Y. Han, Cu embedded Co oxides and its Fenton-like activity for metronidazole degradation over a wide pH range: Active sites of Cu doped Co_3O_4 with $\{112\}$ exposed facet, *Chem. Eng. J.*, 2022, 435, 132910–132921.
- [6] X. Yao, Q. Lin, L. Zeng, J. Xiang, G. Yin, Q. Liu, Degradation of humic acid using hydrogen peroxide activated by $\text{CuO}@ \text{Co}_3\text{O}_4 @ \text{AC}$ under microwave irradiation, *Chem. Eng. J.*, 2017, 330, 783–791.
- [7] L. Lyu, L. Zhang, G. He, H. He, C. Hu, Selective H_2O_2 conversion to hydroxyl radicals in the electron-rich area of hydroxylated C-g- $\text{C}_3\text{N}_4/\text{CuCo-Al}_2\text{O}_3$, *J. Mater. Chem. A*, 2017, 5, 7153–7164.
- [8] M. Xia, M. Long, Y. Yang, C. Chen, W. Cai, B. Zhou, A highly active bimetallic oxides catalyst supported on Al-containing MCM-41 for Fenton oxidation of phenol solution, *Appl. Catal. B: Environ.*, 2011, 110, 118–125.
- [9] L. Lyu, W. Cao, G. Yu, D. Yan, K. Deng, C. Lu, C. Hu, Enhanced polarization of electron-poor/rich micro-centers over $n\text{ZnCu-Cu(II)-rGO}$ for pollutant removal with H_2O_2 , *J. Hazard. Mater.*, 2020, 383, 121182–121191.